



## Original Research Article

### Simulation of Flow in Unconventional Bends to Determine Minor Head Losses and Loss Coefficient using SolidWorks

\*Musa, N.A., Oriaifo, M.A. and Isamotu, O.F.

Department of Mechanical Engineering, Federal University of Technology, Minna, Niger State, Nigeria.

\*madonick1@yahoo.com

#### ARTICLE INFORMATION

##### Article history:

Received 09 November, 2018

Revised 05 December, 2018

Accepted 07 December, 2018

Available online 30 December, 2018

##### Keywords:

Bends

Flow

SolidWorks

Simulations

Pressure loss

Minor head loss

Loss coefficient

#### ABSTRACT

*The aim of this paper is to determine the losses that occur in unconventional bends, which find applications in pipeline networks. Bends of twenty, thirty and sixty degrees were designed in SolidWorks environment and boundary conditions were applied to obtain pressure drops or losses. The pressure drops obtained were used to calculate the minor head loss that occurs in the respective bends and their respective loss coefficient (K). The pipe used was poly vinyl chloride (PVC) pipe with internal diameter of 0.0127m and the working fluid was water. The boundary conditions taken for flow rate was 0.34litres per second (0.00034 m<sup>3</sup>/s), which gave a velocity of 2.688 m/s. From continuity equation and Reynolds number evaluation, it was observed that the flow regimes were turbulent. The minor head loss obtained for 20°, 30° and 60° bends were found to be 0.06440m, 0.06466m and 0.06746m respectively and the corresponding loss coefficient obtained were 0.175, 0.176 and 0.183.*

© 2018 RJEES. All rights reserved.

## 1. INTRODUCTION

Total headloss in a pipeline comprises of major headloss and minor headloss. The former is broadly an energy loss in the pipeline as a result of the effect of resistance to flow of fluid, which largely depends on the fluid viscosity, wall roughness, internal diameter of the pipe, lateral length, and flow velocity (Neto et al., 2014). The latter is the additional energy loss due to secondary flows that are caused by fittings such as bends, elbow, reducers, valves etc. in the pipeline (Neto et al., 2014). Each fitting causes pressure loss or minor head loss which is always expressed as a fraction of the kinetic head (Yildirim, 2010). The evaluation of minor head loss in pipelines network should not be under minded, because in short pipeline fitted with bends and other fittings, minor losses are more than major losses (Liu, 2003). Kamand (1988) stated that the evaluation of total head loss in pipelines is an important factor that affects the overall cost as well as the hydraulic balance of the network.

Bends are used to control and divert flows, when large radius of curvature of diversion of flow is required in flow line. When small radius of curvature of the diversion is required, elbows are used. Conventional bends, that is, bends that are commonly available for use are  $22.5^\circ$ ,  $45^\circ$ ,  $90^\circ$  and  $180^\circ$  bends. If the required angle of diversion of flow is between or above the angle of conventional bends, the use of conventional bends is no longer feasible. Bends of  $20^\circ$ ,  $30^\circ$  and  $60^\circ$  are unconventional bends and they could be respectively employed to divert flow in flow lines that require any angle of diversion of  $20^\circ$ ,  $30^\circ$  and  $60^\circ$ . But there is little or no knowledge about the head loss and loss coefficient (K factor) associated with these unconventional bends in literature. It is the gap this research work seeks to fill by using a viable method to evaluate the head losses and loss coefficients of the unconventional bends.

According to Jonuskaite (2017), fluid flow may be very hard to predict and differential equations that are used in fluid mechanics are difficult to solve but SolidWorks add-ins, enable one to simulate flow of fluid and efficiently analyse the effects of the fluid flow. Hence, in this study, simulation of pressure loss in the various bends was carried out using SolidWorks for the determination of the head loss and the respective loss coefficient of the aforementioned unconventional bends.

## 2. MATERIALS AND METHODS

### 2.1. Materials

The material used in this study include: twenty, thirty and sixty degrees poly vinyl chloride (PVC) bends with each bend having 0.0127m diameter, water which served as the working fluid and it was assumed to be pumped using a 0.5 horse power centrifugal pump to attain a flow rate of 0.34 litre per seconds ( $0.00034 \text{ m}^3/\text{s}$ ), in the bends for the simulation of pressure loss. SolidWorks 2017 software was used for the simulation of pressure loss in the selected bends of  $20^\circ$ ,  $30^\circ$  and  $60^\circ$ .

### 2.2. Methods

The flow chart for the process of determining pressure loss, head loss and loss coefficient of the selected bends is shown in Figure 1.

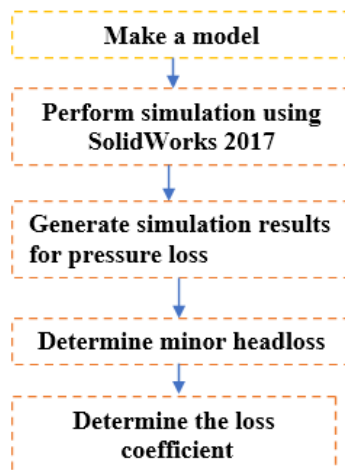


Figure 1: Flow chart for the process of determination of pressure loss, headloss and loss coefficient of the selected bends

**2.2.1. Estimation of fluid flow velocity and Reynold's number**

The flow rate or discharge of fluid is given as:

$$Q = AV \quad (1)$$

Where Q = flow rate = 0.00034 m<sup>3</sup>/s

Area of the pipe used is given as:

$$A = \frac{\pi d^2}{4} \quad (2)$$

Where:

A= area of pipe used

d =pipe diameter (0.0127m)

$$A = \frac{\pi \times 0.0127^2}{4} = 0.000127 \text{ m}^2$$

V= fluid flow velocity

From Equation 1:

$$V = \frac{Q}{A}$$

$$V = 2.688 \text{ m/s}$$

The Reynold's Number (Re) is given as:

$$Re = \frac{\rho V D}{\mu} \quad (3)$$

$\rho$  = Density of fluid (water) = 998.1934 kg/m<sup>3</sup>

V = Velocity of flow = 2.688 m/s

D = Diameter of pipe used = 0.0127 m

$\mu$  = Dynamic viscosity of water from Thermodynamics Table (at 20 °C) = 0.0010016 Pa.s

$$Re = \frac{998.1934 \times 2.688 \times 0.0127}{0.0010016} = 34021.49$$

Since Re is greater than 2000, the flow is entirely turbulent.

**2.2.2. Numerical simulations**

For the calculation of flows in bends, SolidWorks was used to solve for the continuity equation, momentum equation together with the K- $\epsilon$  turbulence model (Cui, 2009).

### 2.2.3 Governing equation and mathematical modeling

According to Nimadge and Chopade (2017), most fluid can be mathematically described by the use of continuity equation and momentum equation (Homicz, 2004). The K-epsilon turbulence model was used to satisfy the boundary layer solution and to generate pressure contours which were analyzed in line with Sharma et al. (2015). Three-dimensional governing equations for steady state, incompressible water flow in cartesian coordinate are given by:

#### Continuity equation:

$$\left(\frac{\partial u}{\partial x} + \frac{\partial v}{\partial y} + \frac{\partial w}{\partial z}\right) = 0 \quad (4)$$

#### Momentum equation:

$$\rho\left(u\frac{\partial u}{\partial x} + v\frac{\partial u}{\partial y} + w\frac{\partial u}{\partial z}\right) = -\frac{\partial p}{\partial x} + \mu\nabla^2 u \quad (5)$$

$$\rho\left(u\frac{\partial v}{\partial x} + v\frac{\partial v}{\partial y} + w\frac{\partial v}{\partial z}\right) = -\frac{\partial p}{\partial y} + \mu\nabla^2 v \quad (6)$$

$$\rho\left(u\frac{\partial w}{\partial x} + v\frac{\partial w}{\partial y} + w\frac{\partial w}{\partial z}\right) = -\frac{\partial p}{\partial z} + \mu\nabla^2 w \quad (7)$$

Where:

- $\rho$  is the density of water
- $p$  is the pressure of water
- $\mu$  is the dynamic viscosity of water
- $x, y, z$  are the cartesian coordinate variables.
- $u, v, w$  are the cartesian velocity components of water

### 2.2.4. Simulation procedure

The SolidWorks 2017 software icon was clicked on the desktop menu on the window interface and a new part was clicked on followed by clicking on the sketch tab which activated all the design tools which were used to design the 20°, 30° and 60° degree bends shown in Figure 2.

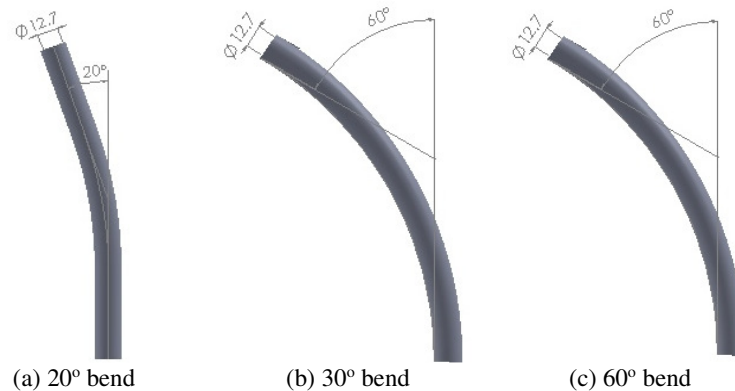


Figure 2: The designed 20°, 30° and 60° bends

After the completion of the design of each bend, exit sketch was clicked on the window interface and design tools were deactivated. The flow simulation tab was checked and all the tools required for simulation were activated and displayed. The wizard option was clicked on to activate a pop-up window. A new project option was clicked on and selection of simulation parameters were displayed. International Standard Organisation (ISO), internal flow, water, adiabatic, 2.68m/s, 20°C and 6000Pa were selected for unit system, analysis type, working fluid, wall condition, velocity, temperature and pressure respectively and the finish icon was clicked on and the computational domain was automatically created around the designed or modelled elbow. Prior to running the simulation, the computational domain was changed to two-dimensional plane. The boundary conditions at inlet and outlet were defined, global goals were selected after which the run icon on the window interface was clicked on. The simulation results were generated which included flow trajectories with fluid pressure contour or distribution and pressure loss in the 20°, 30° and 60° bends respectively.

### 2.2.5. Evaluation of minor headloss and loss coefficient

The minor headlosses and loss coefficients for the 20°, 30° and 60° bend, were evaluated using the relations given by Rajput (2013), Kumar (2014), and Jonuskaite (2017):

$$H_{\text{Bend}} = K \frac{v^2}{2g} = \frac{\Delta P}{\rho g} \quad (8)$$

Where  $H_{\text{Bend}}$  is the minor headloss, K is the loss coefficients, v is the average velocity of fluid in the bend,  $\Delta P$  is the pressure loss or drop, obtained from the simulation result,  $g$  is the acceleration due to gravity and  $\rho$  is fluid density.

## 3. RESULTS AND DISCUSSION

The flow trajectories obtained from the simulation, showing fluid pressure contours or distribution in the 20° bend is shown in Figure 3.

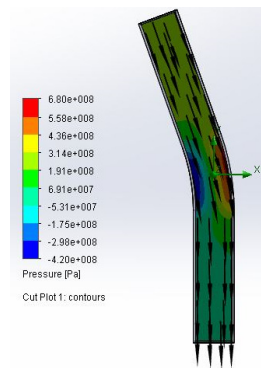


Figure 3: Flow trajectories with fluid pressure contour or distribution in the 20° bend

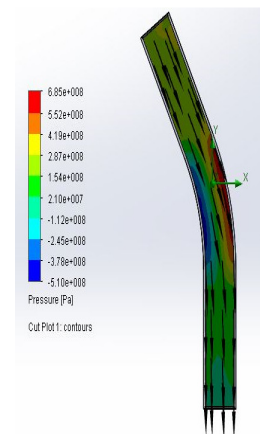


Figure 4: Flow trajectories with fluid pressure contour or distribution in the 30° bend

The different colours in Figure 3, depict different magnitude of the fluid pressure and it can be seen that the fluid pressure varied continuously along the bend. The pressure was maximum at initial point of pipe bend

and decreased across the bend and became minimum at the bend as also experienced and reported by Praveen et al. (2017) in their works. The simulation result for pressure loss in 20° bend is shown in Table 1. It is evident in Table 1 that the total inlet pressure is greater than the total outlet pressure of the fluid in the 20° bend. The simulated pressure loss or simulated total pressure loss obtained for the 20° bend was  $0.0632 \times 10^8$  Pa.

Table 1: Simulation result for pressure loss in 20° bend

S/No	Flow parameter	Unit	Values
1	Total pressure loss	Pa	$0.0631 \times 10^8$
2	Total inlet pressure	Pa	$3.8914 \times 10^8$
3	Total outlet pressure	Pa	$3.8283 \times 10^8$
4	Density	kg/m <sup>3</sup>	998.1934
5	Velocity	m/s	2.6880

The flow trajectories obtained from simulation, showing fluid pressure contour or distribution in the 30° bend is shown in Figure 4. The colour variations in Figure 4, reflect different magnitude of pressure and it can be seen that in the lower part of the 30° bend the fluid pressure dropped continuously. This is because the centrifugal force acting on the fluid flowing through the bend produces a radial pressure gradient which makes a double spiral flow field created by the fluid at the centre of the bend moving towards the outer edge and coming back along the wall towards the inner edge (Enzu, 2015). The simulation result for pressure loss in 30° bend is shown in Table 2.

Table 2: Simulation result for pressure loss in 30° bend

S/No	Flow parameter	Unit	Values
1	Total pressure loss	Pa	$0.0633 \times 10^8$
2	Total inlet pressure	Pa	$3.9085 \times 10^8$
3	Total outlet pressure	Pa	$3.8452 \times 10^8$
4	Density	kg/m <sup>3</sup>	998.1934
5	Velocity	m/s	2.6880

It is clearly seen from Table 2 that the total inlet pressure is greater than the total outlet pressure of the fluid in the 30° bend. The simulated pressure loss or simulated total pressure loss obtained for the 30° bend was  $0.0633 \times 10^8$  Pa. The flow trajectories obtained from simulation, showing fluid pressure contour or distribution in the 60° bend is shown in Figure 5.

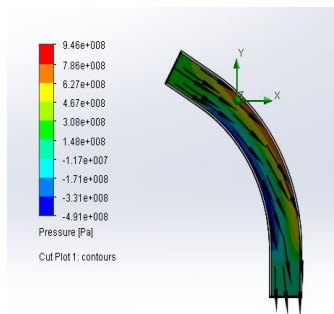


Figure 5: Flow trajectories with fluid pressure contour or distribution in the 60° bend

The contrasting colours in Figure 5, show the different magnitude of pressure and it can be seen that in the lower part of the 60° bend, the fluid pressure dropped continuously and increased again, but in the upper part of the 60° bend, the pressure increased and finally dropped. The drop in pressure was as a result of impact of centrifugal force resulting from the circular motion of the fluid particles induced by the curvature of the pipe bend (Dutta and Nandi, 2016). The simulation result for pressure loss in 60° bend is shown in Table 3.

Table 3: Simulation result for pressure loss in 60° bend

S/No	Flow parameter	Unit	Values
1	Total pressure loss	Pa	0.0661x10 <sup>8</sup>
2	Total inlet pressure	Pa	3.8949x10 <sup>8</sup>
3	Total outlet pressure	Pa	3.8288x10 <sup>8</sup>
4	Density	kg/m <sup>3</sup>	998.1934
5	Velocity	m/s	2.6680

It can be seen from Table 3 that the total inlet pressure is greater than the total outlet pressure of the fluid in the 60° bend. The simulated pressure loss or simulated total pressure loss obtained for the 60° bend was  $0.0661 \times 10^8$  Pa. The result of estimation of minor headloss and loss coefficient of 20°, 30° and 60° bends based on the obtained pressure loss from simulation of flow through the various bends using Equation 8 is shown in Table 4.

Table 4: The evaluated minor headloss and loss coefficient of 20°, 30° and 60° bends

Types of bend	Minor head loss (m)	Loss coefficient (K)
20° bend	0.06440	0.175
30° bend	0.06466	0.176
60° bend	0.06746	0.183

It can be seen from Table 4 that 60° degree elbow has the highest head loss and loss coefficient of 0.06746m and 0.183 respectively, followed by 30° bend having head loss and loss coefficient of 0.06466m and 0.176 respectively. The twenty degree (20°) bend has the lowest head loss and loss coefficient in comparison with others. This result is partly confirmed by the remark made by Islam et al. (2016) based on their works that increase in bending angle increases loss coefficient.

#### 4. CONCLUSION

Simulation of pressure losses in 20°, 30° and 60° bends has been carried out and head losses as well as loss coefficient of the bends have been evaluated in this study. It can be concluded, based on the result of the study, that a higher angle bend experiences greater pressure loss and minor head loss and possesses higher loss coefficient than a lower angle bend.

#### 6. CONFLICT OF INTEREST

There is no conflict of interest associated with this work.

#### REFERENCES

- Cui, J. (2009). Numerical modelling of pressure losses caused by bends in pneumatic conveying pipeline. In: *Proceedings of ASME International Mechanical Engineering Congress and Exposition*, November 13 - 19, Lake Buena Vista, Florida USA.
- Dutta, P and Nandi, N. (2016). Effect of bend curvature on velocity & pressure distribution from straight to a 90° pipe bend - A Numerical Study. *REST Journal on Emerging Trends in Modelling and Manufacturing*, 2(4), pp.103-108.
- Enzu, Z. (2015). Hydrodynamic Simulation of Oil Sand Multiphase Flow in At Face Slurry System. *M.Sc Thesis*, Department of Civil and Environmental Engineering, University of Alberta.
- Homicz, G.F. (2004). *Computational fluid dynamics simulations of pipe elbow flows*. Available electronically at <http://prod.sandia.govt/techlibnauth/access-control.cgi/2004/043467.pdf>. Accessed on April, 2018.
- Islam, M. S., Basak, A., Sarkar, M. A. R. and Islam, M. Q. (2016). Study of minor loss coefficient of flexible pipes for different bend angles and different bend radius by experiment and simulation. *Global Journal of Researches in Engineering: A Mechanical and Mechanics Engineering*, 16(4), pp. 27-32.

- Jonuskaite, A. (2017). Flow Simulation with Solidworks. *B. Tech Thesis*, Arcada University of Applied Sciences, Helsinki, Finland.
- Kamand, F. Z. (1988). Hydraulic friction factors for pipe flow. *Journal of Irrigation and Drainage Engineering*, 114(2), pp. 311-323.
- Kumar, D.S. (2014). *A Textbook of fluid mechanics and fluid power engineering*. India: S.K. Kataria and sons, Publications.
- Liu, H. (2003). *Pipeline Engineering*. New York: CRC Press Company.
- Neto, O.R., Botrel, T.A., Frizzone, J.A. and. Camargo, A.P (2014). Method for determining friction head-loss along elastic pipes. *Irrigation Science*, 32(5), pp. 329-339.
- Nimadge, G.B. and Chopade, S.V. (2017). CFD analysis of flows through T-junction of Pipe. *International research Journal of Engineering and Technology*, 4(2), pp. 906-911.
- Praveen, K., Nitin, K. and Hemant, K. (2017). Numerical investigation of pressure drop and erosion wear by computational fluid dynamics simulation. *International Journal of Mechanical, Aerospace, Industrial, Mechatronic and Manufacturing Engineering*, 11(2), pp. 299-302.
- Rajput, R.K. (2013). *A Text book of fluid mechanics and hydraulic machine in SI Unit*. New Delhi, S. Chand and company limited.
- Sharma, A.S., Sudhakar, S., Akumar, S and. Kumar, B.S. (2015). Investigations of pressure contours and velocity vectors of NACA 0015 using Gurney Flap. *International Journal of Mechanical and Production Engineering*, 3(9), pp. 12-16.
- Yildirim, G. (2010). Total energy loss assessment for trickle lateral lines equipped with integrated in-line and on-line emitters. *Irrigation Science*, 28(4), pp. 341–352.